Synthesis, Crystal structure, and Magnetic Properties of Dinuclear Iron(III) Complexes with Methoxo Bridges

Jong Won Shin,[†] Jeong Hyeong Han, Sankara Rao Rowthu,[†] Bong Gon Kim,[‡] and Kil Sik Min[*]

Department of Chemistry Education, Kyungpook National University, Daegu 702-701, Korea. [*]E-mail: minks@knu.ac.kr
[†]Department of Chemistry, Kyungpook National University, Daegu 702-701, Korea
[‡]Department of Chemistry Education, Gyeongsang National University, Jinju 660-701, Korea

The reaction of stoichiometric amount of $FeCl_2 \cdot 4H_2O$, (2-pyridylmethyl, 3-pyridylmethyl)amine (2,3-pyma) and sodium azide/sodium thiocyanate in methanol under aerobic conditions affords the dinuclear Fe(III) complexes, $[(2,3\text{-pyma})(N_3)_2Fe(\mu\text{-}OCH_3)_2Fe(N_3)_2(2,3\text{-pyma})] \cdot CH_3OH$ (**1**) and $[(2,3\text{-pyma})(NCS)_2Fe(\mu\text{-}OCH_3)_2Fe(NCS)_2(2,3\text{-pyma})]$ (**2**) in good yield. Two bis-methoxy-bridged diiron(III) complexes are isolated and characterized. The coordination geometries around iron(III) ions in **1** and **2** are the same tetragonally distorted octahedron. The iron(III) ions are coordinated by two nitrogens of a 2,3-pyma, two nitrogens of two azide/thiocyanate ions, and two oxygens of two methoxy groups. Both compounds are isomorphous. The structures of **1** and **2** display the C-H···π and/or π-π stacking interactions as well as hydrogen bonding interactions, respectively. Compounds **1** and **2** show significant antiferromagnetic couplings through the bridged methoxy groups between the iron(III) ions in the temperature range from 5 to 300 K ($H = -2JS_1 \cdot S_2$, $J = -19.1$ and -13.9 cm^{-1} for **1** and **2**).

Key Words: Iron(III) complex, Ligand, Crystal structure, Stacking interactions, Magnetic properties

Introduction

The design and synthesis of discrete multinuclear metal complexes continue to be a research area of increasing importance due to the structural elucidation of metal centers in biomimetic model for metalloenzymes and the potential applications such as molecule-based magnetism and redox catalysis.[1] Among these studies, many iron(III) and copper(II) dinuclear complexes with bis(μ-alkoxo)-bridged linkages have been investigated, in order to characterize the superexchange couplings *via* the alkoxo ligands between the metal ions.[2] For examples, the diiron(III) complexes, $[PH(t\text{-}Bu)_3]_2[Fe_2(\mu\text{-}OEt)_2Cl_6]$ and $Fe_2(pesd)(\mu\text{-}OCH_3)_2Cl_2$, have been shown the antiferromagnetic interactions with coupling constants (*J*) of -24.6 and -16.3 cm^{-1}, respectively (pesd = 1,4-piperazinediylbis(*N*-ethylenesalicylaldiminato)).[3] Furthermore, a bis(μ-alkoxo)-bridged dinuclear iron(III) complex with a tripodal N3O ligand, $[Fe(pmha)(NO_3)_2]_2(NO_3)_2$ (Hpmha = *N*,*N*-bis(2-pyridylmethyl)-*N*-(2-hydroxyethyl)amine), was prepared as a biomimetic model for the dioxygenase enzymes and showed the intradiol-cleaving dioxygenase activity.[4] Very recently, a tetranuclear iron(III) complex bridged with methoxy groups and azide ions has been prepared and interestingly it showed both ferromagnetic and antiferromagnetic interactions within the discrete unit.[5] In this context, we tried to explore to make discrete iron(III) dinuclear complexes bridged with end-on azide ions displaying a ferromagnetic coupling. Unexpectedly, we have obtained two bis(μ-OCH_3)-bridged iron(III) dinuclear complexes, not the sought end-on azido-bridged diiron(III) complexes, i.e., $[(2,3\text{-pyma})(N_3)_2Fe(\mu\text{-}1,1\text{-}N_3)_2Fe(N_3)_2(2,3\text{-pyma})]$. Herein, we report the synthesis, crystal structures, and magnetic properties of bis(μ-OCH_3)-bridged iron(III) dinuclear complexes, $[(2,3\text{-pyma})(N_3)_2Fe(\mu\text{-}OCH_3)_2Fe(N_3)_2(2,3\text{-pyma})] \cdot CH_3OH$ (**1**) and $[(2,3\text{-pyma})(NCS)_2Fe(\mu\text{-}OCH_3)_2$

$Fe(NCS)_2(2,3\text{-pyma})]$ (**2**), prepared from the reaction of $FeCl_2 \cdot 4H_2O$, 2,3-pyma, and $NaN_3/NaSCN$ in methanol.

Experimental Section

Materials and measurements. All chemicals and solvents used in the syntheses were of reagent grade and were used without further purification. (2-pyridylmethyl, 3-pyridylmethyl)amine (2,3-pyma, $C_{12}H_{12}N_3$) was prepared by a literature method.[6] Infrared spectra were recorded with a ThermoFisher Scientific IR200 FT-IR spectrometer (± 1 cm^{-1}). Elemental analyses were performed by the analytical laboratory of Kyungpook National University. Magnetic susceptibilities were measured in an applied field of 5000 Oe between 5 and 300 K on a Quantum Design MPMS superconducting quantum interference device (SQUID) magnetometer. Diamagnetic corrections were made by using Pascal's constants (522 (**1**) and 486×10^{-6} emu/mol (**2**)).

Preparation of $[(2,3\text{-pyma})(N_3)_2Fe(\mu\text{-}OCH_3)_2Fe(N_3)_2(2,3\text{-pyma})] \cdot CH_3OH$ (1). To a MeOH solution (10 mL) of $FeCl_2 \cdot 4H_2O$ (50 mg, 0.25 mmol) was added dropwise a MeOH solution (10 mL) of (2-pyridylmethyl, 3-pyridylmethyl)amine (2,3-pyma, 50 mg, 0.25 mmol), and the color became dark red, and the solution was stirred for 30 min at room temperature. A MeOH solution (10 mL) of sodium azide (33 mg, 0.51 mmol) was added to the mixture solution and the solution was allowed to stir for 2 h. Red precipitates of **1** formed that collected by filtration and washed with methanol, and dried in air. Yield: 70 mg (69%). Single crystals of **1** suitable for X-ray crystallography were obtained from a DMF/MeOH (v/v, 1:4) mixture solution. IR (KBr) 3378, 3253, 2941, 2916, 2818, 2070, 2047, 1608, 1342, 1031 cm^{-1}. Anal. Calcd for $C_{28}H_{40}Fe_2N_{18}O_4$: C, 41.81; H, 5.01; N 31.34. Found: C, 41.49; H, 4.77; N, 31.00.

Preparation of $[(2,3\text{-pyma})(NCS)_2Fe(\mu\text{-}OCH_3)_2Fe(NCS)_2$

(2,3-pyma)] (2). To a MeOH solution (10 mL) of $FeCl_2 \cdot 4H_2O$ (50 mg, 0.25 mmol) was added dropwise a MeOH solution (10 mL) of 2,3-pyma (50 mg, 0.25 mmol), and the color became dark red, and the solution was stirred for 30 min at room temperature. A MeOH solution (10 mL) of sodium thiocyanate (41 mg, 0.51 mmol) was added to the mixture solution and the solution was allowed to stir for 2 h. Red precipitates of **2** formed that collected by filtration and washed with methanol, and dried in air. Yield: 53 mg (49%). Single crystals of **2** suitable for X-ray crystallography were obtained from a DMF/MeOH (v/v, 1:4) mixture solution. IR (KBr) 3203, 3129, 2953, 2887, 2819, 2035, 2012(sh), 1607, 1480, 1034 cm^{-1}. Anal. Calcd for $C_{32}H_{40}$-$Fe_2N_{10}S_4O_4$: C, 44.24; H, 4.64; N 16.12; S, 14.77. Found: C, 44.26; H, 4.34; N, 16.16; S, 14.27.

X-ray crystallographic data collection and refinement. Single crystals of **1** and **2** were mounted on a Bruker SMART APEX CCD-based diffractometer (Korea Basic Science Institute, Chonju Branch). X-ray data for **1** and **2** were collected at 173(2) K and using Mo Kα radiation ($\lambda = 0.71073$ Å, graphite monochromator). The raw data were processed to give structure factors using the Bruker SAINT program and corrected for Lorentz and polarization effects.[7] For **1** and **2**, the intensity data were corrected for absorption using SADABS program with multi-scan data ($T_{max}/T_{min} = 0.857$ for **1** and 0.885 for **2**).[8] The crystal structures were solved by direct methods,[9] and refined by full-matrix least-squares refinement using the SHELXL97

computer program.[10] All non-hydrogen atoms were refined anisotropically. All hydrogen atoms except for CH_3OH were positioned geometrically and refined using a riding model. The crystallographic data and the result of refinements are summarized in Table 1.

Results and Discussion

Synthesis and characterization. The reaction of 1 equiv of 2,3-pyma and $FeCl_2 \cdot 4H_2O$ and 2 equiv of NaN_3 or NaSCN in MeOH solution under aerobic conditions affords the dinuclear complexes, $[(2,3\text{-pyma})(N_3)_2Fe(\mu\text{-OCH}_3)_2Fe(N_3)_2(2,3\text{-pyma})]\cdot CH_3OH$ (**1**) and $[(2,3\text{-pyma})(NCS)_2Fe(\mu\text{-OCH}_3)_2Fe(NCS)_2(2,3\text{-pyma})]$ (**2**) in moderate yield, respectively. Interestingly, bis-methoxy-bridged diiron(III) compounds are obtained. As shown in X-ray crystal structures (vide infra), both iron (III) ions in **1** and **2** are connected by oxygen atoms of two methoxy groups resulted from methanol molecules, not the sought azido- or thiocyanto-bridged dinuclear complex, i.e. $[(2,3\text{-pyma})Fe(\mu\text{-N}_3)_2Fe(2,3\text{-pyma})]^{n+}$ or $[(2,3\text{-pyma})Fe(\mu\text{-NCS})_2Fe(2,3\text{-pyma})]^{n+}$ dinuclear units. The compositions of **1** and **2** were determined by elemental analysis, infrared, and X-ray diffraction. The IR spectrum (KBr pellet) of **1** shows $\nu_{N\equiv N}$ of the azide ions at 2070 and 2047 cm^{-1} and ν_{NH} of the 2,3-pyma at 3253 cm^{-1}.[11] The IR spectrum (KBr pellet) of **2** shows $\nu_{C\equiv N}$ of the thiocyanate ions at 2035 and 2012 cm^{-1} and ν_{NH} of the 2,3-pyma at 3203 cm^{-1}.[11] Both compounds display the peaks corresponding to the methoxy groups at 2941, 2916, and 2818 for **1** and 2953, 2887, and 2819 cm^{-1} for **2**, respectively.

X-ray crystal structure of $[(2,3\text{-pyma})(N_3)_2Fe(\mu\text{-OCH}_3)_2Fe(N_3)_2(2,3\text{-pyma})]\cdot CH_3OH$ (1). An ORTEP drawing of **1** is shown in Figure 1 and selected bond distances and angles are listed in Table 2. The coordination geometry around iron(III) ion is a tetragonally distorted octahedron. The iron(III) ion is coordinated with two nitrogens of a 2,3-pyma, two nitrogens of two azide ions, and two oxygens of two methoxy groups. The aver-

Table 1. Summary of the crystallographic data for **1** and **2**

	1	**2**
formula	$C_{27}H_{36}Fe_2N_{18}O_3$	$C_{30}H_{32}Fe_2N_{10}O_2S_4$
M_r	772.44	804.60
crystal system	monoclinic	triclinic
space group	$C2/c$	$P\bar{1}$
a, Å	26.047(6)	8.046(3)
b, Å	9.903(2)	10.464(4)
c, Å	15.661(4)	11.042(4)
α, deg	90	97.004(8)
β, deg	121.244(4)	102.220(8)
γ, deg	90	102.726(7)
V, Å^3	3453.5(14)	872.3(6)
Z	4	1
D_{calc},	1.486	1.532
T, K	173(2)	173(2)
λ, Å	0.71073	0.71073
μ, mm^{-1}	0.899	1.116
$F(000)$	1600	414
collected	12080	6413
unique	4228	4189
observed	3150	2526
parameters	228	219
GOF	1.116	1.108
R_1 (4α data)^a	0.0436	0.0734
wR_2 (4α data)^b	0.1050	0.1888

$^a R_1 = \Sigma ||F_o| - |F_c||/\Sigma|F_o|$. $^b wR_2 = [\Sigma w(F_o^2 - F_c^2)^2/\Sigma w(F_o^2)^2]^{1/2}$.

Figure 1. Structure of the $[(2,3\text{-pyma})(N_3)_2Fe(\mu\text{-OCH}_3)_2Fe(N_3)_2(2,3\text{-pyma})]\cdot CH_3OH$ (**1**). The atoms are represented by 30% probable thermal ellipsoids. Hydrogen atoms and CH_3OH are omitted for clarity (' = 0.5-x, 1.5-y, 1-z).
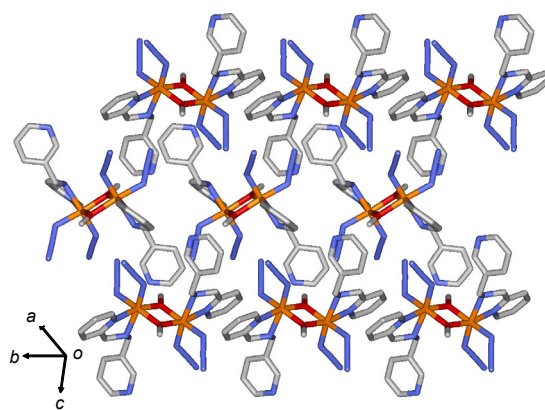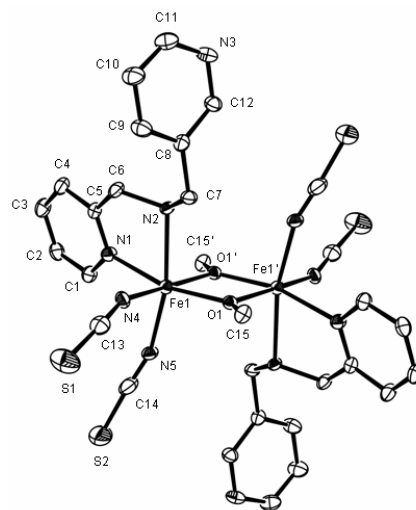
Table 2. Selected Bond Distances (Å) and Angles (deg) for **1** and **2**

[(2,3-pyma)(N₃)₂Fe(μ-OCH₃)₂Fe(N₃)₂(2,3-pyma)]·CH₃OH (**1**)			
Fe1-N1	2.189(3)	Fe1-N7	2.016(3)
Fe1-N2	2.188(3)	Fe1-O1	2.005(2)
Fe1-N4	2.018(3)	Fe1-O1^i	1.974(2)
Fe1-Fe1^i	3.137(1)	N7-N8	1.169(4)
N4-N5	1.191(4)	N8-N9	1.153(5)
N5-N6	1.156(4)	O1-C13	1.422(4)
N1-Fe1-N2	74.96(10)	N2-Fe1-O1^i	94.65(9)
N1-Fe1-N4	91.43(11)	N4-Fe1-N7	94.16(13)
N1-Fe1-N7	93.42(12)	N4-Fe1-O1	170.88(11)
N1-Fe1-O1	93.88(9)	N4-Fe1-O1^i	97.49(11)
N1-Fe1-O1^i	165.69(10)	N7-Fe1-O1	92.93(11)
N2-Fe1-N4	84.79(10)	N7-Fe1-O1^i	97.05(11)
N2-Fe1-N7	168.29(11)	O1-Fe1-O1^i	75.92(9)
N2-Fe1-O1	89.43(9)	Fe1-O1-Fe1^i	104.08(9)
[(2,3-pyma)(NCS)₂Fe(μ-OCH₃)₂Fe(NCS)₂(2,3-pyma)] (**2**)			
Fe1-N1	2.175(4)	Fe1-N5	2.063(5)
Fe1-N2	2.228(4)	Fe1-O1	1.974(4)
Fe1-N4	2.067(5)	Fe1-O1^{ii}	1.999(4)
Fe1-Fe1^{ii}	3.141(2)	N5-C14	1.107(8)
N4-C13	1.121(8)	C14-S2	1.630(8)
C13-S1	1.607(7)	O1-C15	1.420(6)
N1-Fe1-N2	75.61(16)	N2-Fe1-O1^{ii}	89.93(15)
N1-Fe1-N4	95.26(18)	N4-Fe1-N5	93.0(2)
N1-Fe1-N5	90.38(18)	N4-Fe1-O1	96.16(17)
N1-Fe1-O1	164.19(17)	N4-Fe1-O1^{ii}	170.64(17)
N1-Fe1-O1^{ii}	92.16(16)	N5-Fe1-O1	99.88(16)
N2-Fe1-N4	86.42(18)	N5-Fe1-O1^{ii}	92.59(17)
N2-Fe1-N5	165.86(16)	O1-Fe1-O1^{ii}	75.50(16)
N2-Fe1-O1	94.22(15)	Fe1-O1-Fe1^{ii}	104.50(16)

Symmetry transformations used to generate equivalent atoms: (i) 0.5-x, 1.5-y, 1-z; (ii) -x, -y, 1-z.

Figure 2. View of CH···π interactions between methyl and pyridine groups in **1**.

Figure 3. Structure of the [(2,3-pyma)(NCS)₂Fe(μ-OCH₃)₂Fe(NCS)₂(2,3-pyma)] (**2**). The atoms are represented by 30% probable thermal ellipsoids. Hydrogen atoms are omitted for clarity (′ = -x, -y, 1-z).

age Fe-N$_{2,3\text{-pyma}}$, Fe-N$_{azido}$, and Fe-O$_{methoxo}$ bond distances are 2.189(2), 2.017(2), and 1.990(1) Å, respectively. The bite distance and angle of the five-membered chelate ring are 2.663(4) Å and 74.96(10)°, respectively. The two iron(III) ions within the dinuclear unit are connected by two methoxy groups with an inversion center. The angles of Fe1-O1-Fe1(0.5-x, 1.5-y, 1-z) and O1-Fe1-O1(0.5-x, 1.5-y, 1-z) are 104.08(9) and 75.92(9)°, respectively. The shortest Fe···Fe contact within the dimer is 3.137(1) Å and the shortest Fe···Fe distance between the dimers is 7.306(2) Å. In the structure of **1**, pyridine pendant groups undergo the C-H···π interactions with the bridged methoxy groups, which propagate along the *c* axis (Figure 2). For the C-H···π interaction, the distance between the centroid of the pyridine pendant ring and the nearest carbon atom of the methoxy group is 3.583 Å (∠C13-H···centroid 85.29 - 101.26°).[12] Furthermore, the secondary nitrogen atom of 2,3-pyma forms hydrogen bonds with the uncoordinated nitrogen atom of azide ion (N2···N6(x, -y+2, z-0.5) 3.125(4) Å, ∠N2-H2-N6 138.68°).

X-ray crystal structure of [(2,3-pyma)(NCS)₂Fe(μ-OCH₃)₂

Fe(NCS)₂(2,3-pyma)] (2). An ORTEP drawing of **2** is shown in Figure 3 and selected bond distances and angles are listed in Table 2. The coordination geometry around iron(III) ion is a tetragonally distorted octahedral structure. The iron(III) ion is coordinated to two nitrogens of a 2,3-pyma, two nitrogens of two thiocyanate ions, and two oxygens of two methoxy groups. The average Fe-N$_{2,3\text{-pyma}}$, Fe-N$_{thiocyanato}$, and Fe-O$_{methoxo}$ bond distances are 2.202(3), 2.065(4), and 1.987(3) Å, respectively. The bite distance and angle of the five-membered chelate ring are 2.700(6) Å and 75.61(16)°, respectively. Similar to **1**, the two iron(III) ions within the dinuclear unit are connected by two methoxy groups. The angles of Fe1-O1-Fe1(-x, -y, 1-z) and O1-Fe1-O1(-x, -y, 1-z) are 104.50(16) and 75.50(16)°, respectively. The crystal structures of **1** and **2** are isomorphous. The shortest Fe···Fe contact within the dimer is 3.141(2) Å and the shortest Fe···Fe distance between the dimers is 8.046(3) Å. In the structure of **2**, two pyridine groups of the 2,3-pyma ligand experience offset π-π stacking interactions with pyridine groups belonging to a neighboring dinuclear complex (Figures 4 and 5).[12] For the
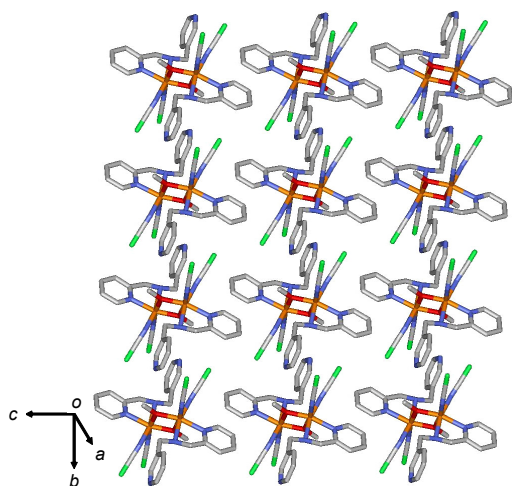
**Figure 4.** View of π-π interactions between the coordinated pyridine groups in **2**.
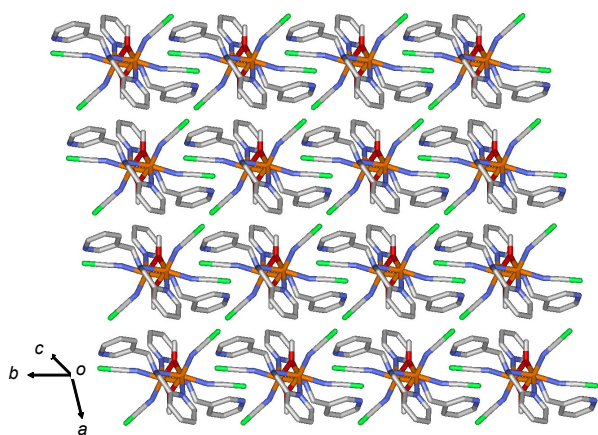
Figure 5. View of π-π interactions between the pendant pyridine groups in **2**.

π-π stacking interactions, the dihedral angle between two pyridine planes coordinated to iron(III) ion is $\theta = 0.0$ deg and the interplanar separation of the aromatic rings is 3.36 - 3.38 Å as well as the offset angle between the ring planes is 20.3° (centroid⋯centroid 3.628 Å) (Figure 4). Additionally, the dihedral angle between the pyridine planes of pendant groups is $\theta = 0.0$ deg and the interplanar separation of the aromatic rings is 3.711 - 3.73 Å as well as the offset angle between the ring planes is 17.9° (centroid⋯centroid 3.919 Å) (Figure 5). In case of **2**, due to the offset π-π stacking interactions, the structure becomes a two-dimensional network. In addition to, the secondary nitrogen atom of 2,3-pyma is involved in a hydrogen-bonding interaction with the nitrogen atom of pyridine pendant group (N2⋯N3 (-x, -y-1, -z+1) 3.138(7) Å, ∠ N2-H2-N3 160.77°).

Magnetic properties. Variable-temperature 5 - 300 K magnetic susceptibility, χ, measurements on solid samples of **1** and **2** have been performed on a SQUID magnetometer (external field 5000 Oe). For complex **1**, at room temperature, the effective magnetic moment, $\mu_{eff} [= (8\chi_M T)^{1/2}]$, is 5.84 μ_B/Fe$_2$. This value is less than the spin-only value of 8.37 μ_B/Fe$_2$ expected for inde-
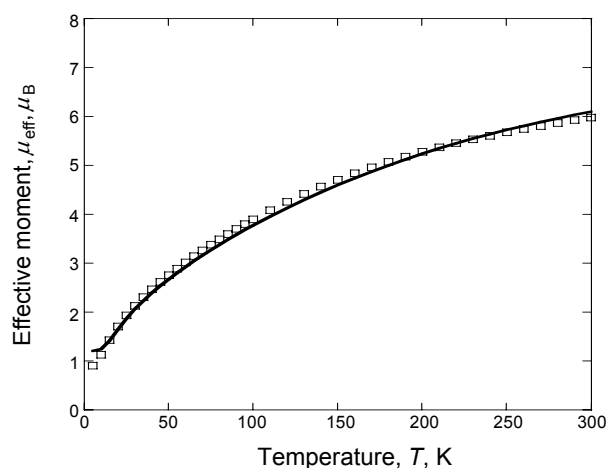
Figure 6. Fitting of effective magnetic moment *versus* temperature (K) data of **1** using dimer model of $S = 5/2$ local spin. Solid line shows the best fit obtained.
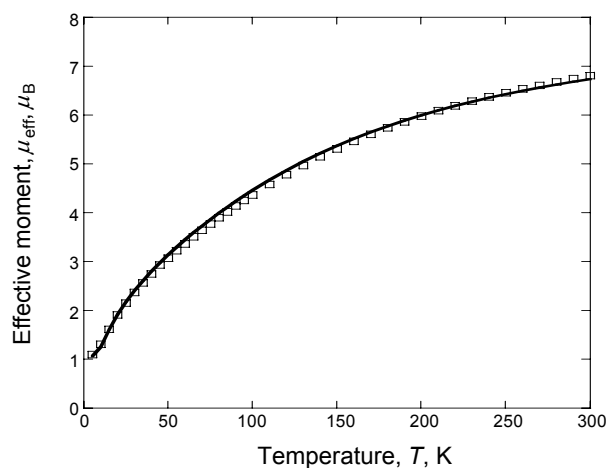
Figure 7. Fitting of effective magnetic moment *versus* temperature (K) data of **2** using dimer model of $S = 5/2$ local spin. Solid line shows the best fit obtained.

pendent two Fe^{III} spins ($g = 2$, $S = 5/2$) indicative of significant antiferromagnetic coupling. $\mu_{eff}(T)$ decreases with decreasing temperature (Figure 6) consistent with the presence of an antiferromagnetic interaction between the Fe(III) ions. The $\mu_{eff}(T)$ data were fit to an analytical expression for $\chi(T)$ for a coupled $S = 5/2$ dinuclear spin model (Eq. (1)) based on the Hamiltonian $H = -2JS_1 \cdot S_2$ ($S_1 = S_2 = 5/2$).[13] The best fit to Eq. (1) had $J = -19.1$ cm^{-1}, $g = 1.99$, and spin impurities, $\rho = 0.021$.

$$\chi_M = \frac{N\beta^2 g^2}{3kT} \left[\frac{6\exp(2J/kT) + 30\exp(6J/kT) + 84\exp(12J/kT) + 180\exp(20J/kT) + 330\exp(30J/kT)}{1 + 3\exp(2J/kT) + 5\exp(6J/kT) + 7\exp(12J/kT) + 9\exp(20J/kT) + 11\exp(30J/kT)} \right](1-\rho) + 2\rho\left[\frac{N\beta^2 g^2}{3kT} S(S+1)\right]$$

(1)

Complex **2** has a room temperature μ_{eff} of 6.68 μ_B/Fe$_2$. The

Table 3. Comparison of Magnetic Properties of Diferric Complexes with Bis(μ-alkoxo) Fe_2O_2 Cores.

Compounds[a]	J (cm^{-1})	g	ρ (%)	Ref.
[(2,3-pyma)(N$_3$)$_2$Fe(μ-OCH$_3$)$_2$Fe(N$_3$)$_2$(2,3-pyma)] (**1**)	−19.1	1.99	2.1	this work
[(2,3-pyma)(NCS)$_2$Fe(μ-OCH$_3$)$_2$Fe(NCS)$_2$(2,3-pyma)] (**2**)	−13.9	2.0	1.6	this work
[Fe$_2$(dbe)$_2$(bz)$_2$](ClO$_4$)$_2$]	−20.5	2.05	0.92	2e
[Fe$_2$(pesd)(μ-OCH$_3$)$_2$Cl$_2$]	−16.3	2.0	6.5	3a
[Fe$_2$(pesd)(μ-OCH$_2$CH$_3$)$_2$Cl$_2$]	−15.4	2.0	1.3	2a
[Fe$_2$(acac)$_4$(μ-OCH$_2$CH$_3$)$_2$Cl$_2$]	−11.0	2.0		2a
[PH(*t*-Bu)$_3$]$_2$[Fe$_2$(μ-OEt)$_2$Cl$_6$]	−24.6	2.0	3.2	3b

[a]abbreviation used: dbe = 2-[bis(2-benzimidazolylmethyl)amino]ethanolato; bz = benzoate; pesd = 1,4-piperazinediylbis(*N*-ethylenesalicylaldiminato); acac = acetylacetonato.

effective magnetic moment is lower than the spin-only value, indicative of antiferromagnetic coupling between the high-spin Fe(III) ions. Likewise **1**, $\mu_{\text{eff}}(T)$ decreases with decreasing temperature (Figure 7) indicative of a strong antiferromagnetic interaction. The $\mu_{\text{eff}}(T)$ data was fit to an analytical expression for $\chi(T)$ for a coupled $S = 5/2$ dinuclear spin model (Eq. (1)). The best fit to Eq. (1) had $J = -13.9$ cm^{-1}, $g = 2.0$, and spin impurities, $\rho = 0.016$.

It should be note that the J values of **1** and **2** indicate that the methoxo groups mediate antiferromagnetic couplings between two iron(III) ions separated by *ca.* 3.14 Å. The coupling constants of **1** and **2** are compared with other alkoxo-bridged diiron(III) compounds in Table 3. Since the methyl group is more electron donating than hydrogen, the more negative J value for methoxy-bridged Fe(III) dinuclear compound than for hydroxyl-bridged Fe(III) dimer observed.[14] As mentioned above, complex **1** has more negative J value for **2**, although complexes **1** and **2** are linked by the same methoxy groups between the iron(III) ions. This can be explained by structural aspects. The bond length of Fe-Fe within the dinuclear unit in **1** is slightly shorter than that of **2** (See Table 2). Due to the short distance, the magnetic coupling of **1** can be occurred more stronger that of **2**.[2a] Furthermore, the angles of Fe1-O1-Fe1′ in **1** and **2** are 104.08(9) and 104.50(16)°, respectively. The latter shows slightly a larger bridging angle *ca.* ~0.42°, indicative of a less negative J value.[2a,3a] However, the average Fe-O$_{\text{methoxo}}$ bond distances for **1** and **2** are 1.990(1) and 1.987(3) Å, respectively. These values are nearly similar within experimental errors. Thus this can be neglected regarding the strength of magnetic interactions. Additionally, the average Fe-L$_N$ bond distance in **1** is shorter than that of **2** about 0.09 Å. That is, this can be facilitated to interact between the Fe(III) ions by an efficient electron donating character, in which the interaction in **1** will be more negative than that of **2**. However, the extent of antiferromagnetic interactions in **1** and **2** is significantly smaller than for oxo-bridged Fe(III) complexes (−J = 80 - 120 cm^{-1}) but is comparable to those found in dihydroxo-bridged Fe(III) dinuclear compounds (−J = 7 - 17 cm^{-1}).[15]

Conclusions

New iron(III) dinuclear complexes bridged with methoxy groups, [(2,3-pyma)(N$_3$)$_2$Fe(μ-OCH$_3$)$_2$Fe(N$_3$)$_2$(2,3-pyma)]·CH$_3$OH (**1**) and [(2,3-pyma)(NCS)$_2$Fe(μ-OCH$_3$)$_2$Fe(NCS)$_2$(2,3-

pyma)] (**2**) have been synthesized and characterized. Both compounds are isomorphous. That is, the iron(III) ions are coordinated by two nitrogens of a 2,3-pyma, two nitrogens of two azide/thiocyanate ions, and two oxygens of two methoxy groups. Additionally the packing structures of **1** and **2** exhibit the C-H···π/π-π stacking interactions and hydrogen bonding interactions. Compounds **1** and **2** show significant antiferromagnetic couplings due to direct spin exchange *via* the bridged methoxy groups. The interaction in **1** is slightly stronger than that of **2**.

Supporting Information. Crystallographic data (excluding structure factors) for the structures reported in this paper have been deposited with the Cambridge Crystallographic Data Centre as supplementary publication nos. CCDC-790595 (for **1**) and CCDC-790594 (for **2**). Copies of the data can be obtained free of charge on application to CCDC, 12 Union Road, Cambridge CB2 1EZ, UK [Fax (internat.) +44-1223/336-033; E-mail: deposit@ccdc.cam.ac.uk].

References

1. (a) Kitagawa, S.; Kawata, S. *Coord. Chem. Rev.* **2002**, *224*, 11. (b) Tshuva, E. Y.; Lippard, S. J. *Chem. Rev.* **2004**, *104*, 987. (c) Benelli, C.; Gatteschi, D. *Chem. Rev.* **2002**, *102*, 2369. (d) Min, K. S.; DiPasquale, A. G.; Golen, J. A.; Rheingold, A. L.; Miller, J. S. *J. Am. Chem. Soc.* **2007**, *129*, 2360. (e) Zilbermann, I.; Maimon, E.; Cohen, H.; Meyerstein, D. *Chem. Rev.* **2005**, *105*, 2609. (f) Tao, J.; Maruyama, H.; Sato, O. *J. Am. Chem. Soc.* **2006**, *128*, 1790.
2. (a) Chiari, B.; Piovesana, O.; Tarantelli, T.; Zanazzi, P. F. *Inorg. Chem.* **1984**, *23*, 3398. (b) Ruiz, E.; Alemany, P.; Alvarez, S.; Cano, J. *Inorg. Chem.* **1997**, *36*, 3683. (c) Ruiz, E.; Alemany, P.; Alvarez, S.; Cano, J. *J. Am. Chem. Soc.* **1997**, *119*, 1297. (d) Ménage, S.; Que, L., Jr. *Inorg. Chem.* **1990**, *29*, 4293. (e) Han, J. H.; Shin, J. W.; Min, K. S. *Bull. Korean Chem. Soc.* **2009**, *30*, 1113.
3. (a) Chiari, B.; Piovesana, O.; Tarantelli, T.; Zanazzi, P. F. *Inorg. Chem.* **1982**, *21*, 1396. (b) Walker, J. D.; Poli, R. *Inorg. Chem.* **1990**, *29*, 756.
4. Li, F.; Wang, M.; Li, P.; Zhang, T.; Sun, L. *Inorg. Chem.* **2007**, *46*, 9364.
5. Shin, J. W.; Rowthu, S. R.; Kim, B. G.; Min, K. S. *Dalton Trans.* **2010**, *39*, 2765.
6. Soibinet, M.; Déchamps-Oliver, I.; Mohamadou, A.; Aplincourt,

M. *Inorg. Chem. Commun.* **2004**, *7*, 405.

7. *Saint Plus*, v. 6.02; Bruker Analytical X-ray: Madison, WI, 1999.

8. Sheldrick, G. M. *SADABS: Siemens/Bruker Area Detector Absorption Correction Program*, V2.03; University of Göttingen: Germany, 2000.

9. Sheldrick, G. M. *Acta Crystallogr., Sect. A* **1990**, *46*, 467.

10. Sheldrick, G. M. *SHELXL97: Program for the Crystal Structure Refinement*; University of Göttingen: Germany, 1997.

11. Nakamoto, K. *Infrared and Raman Spectra of Inorganic and Coordination Compounds*; WILEY: New Jersey, 2009; pp 120-131.

12. (a) Desiraju, G. R. *Crystal Engineering: The Design of Organic Solids*; Elsevier: New York, 1989; Chap. 4. (b) Shetty, A. S.;

Zhang, J.; Moore, J. S. *J. Am. Chem. Soc.* **1996**, *118*, 1019. (c) Jennings, W. B.; Farrell, B. M.; Malone, J. F. *Acc. Chem. Res.* **2001**, *34*, 885.

13. Kahn, O. *Molecular Magnetism*; VCH: New York, 1993; pp 103-134.

14. Chiari, B.; Piovesana, O.; Tarantelli, T.; Zanazzi, P. F. *Inorg. Chem.* **1983**, *22*, 2781.

15. (a) Kato, M.; Yamada, Y.; Inagaki, T.; Mori, W.; Sakai, K.; Tsubomura, T.; Sato, M.; Yano, S. *Inorg. Chem.* **1995**, *34*, 2645. (b) Ghiladi, M.; Larsen, F. B.; McKenzie, C. J.; Søtofte, I.; Tuchagues, J.-P. *Dalton Trans.* **2005**, 1687. (c) Min, K. S.; Arif, A. M.; Miller, J. S. *Inorg. Chim. Acta* **2007**, *360*, 1854.